

---

# Mechanical Properties of Polycarbonate–Polysulfone and Polycarbonate–Polyetherimide Blends

---

**WILLIAM G. KOHLMAN\***

*U.S. Army Natick Research, Development, and Engineering Center, Kansas Street, Natick,  
Massachusetts 01760-5020*

**STEPHEN P. PETRIE**

*Department of Plastics Engineering, University of Massachusetts Lowell, One University Avenue,  
Lowell, Massachusetts 01854*

## ABSTRACT

---

Five, ten, and twenty percent by weight blends of polysulfone in polycarbonate and polyetherimide in polycarbonate were produced by melt blending. The materials were injection molded into plaques. Mechanical analysis consisting of tensile, pendulum impact, and ballistic impact testing was conducted using the plaques or samples machined from the plaques. The average impact strength and percentage of ductile failures decreased with increasing composition of polysulfone and polyetherimide. The tensile test results indicate that a relationship exists between the percent composition and the yield strength for the blends with the blends showing an improvement in tensile strength. The ballistic testing results show that a possibly linear relationship exists between the percent composition and the critical velocity for complete penetration. Differential scanning calorimetry was conducted to measure the glass transition temperatures of the materials. The presence of two glass transition temperatures and lack of transparency have indicated that the blends are immiscible. © 1995 John Wiley & Sons, Inc.

\* To whom correspondence should be addressed.

This article reports research sponsored by the U.S. Army Natick Research, Development and Engineering Center and has been assigned TP-3430 in the series of papers approved for publication.

## Introduction

**B**isphenol A polycarbonate is an extremely tough transparent engineering thermoplastic.<sup>1</sup> The Izod impact strength for polycarbonate is 640 to 860 J/m of notch. A failing of polycarbonate is its liability to crack or craze under strain or exposure to various solvents. The polymer is also relatively soft. The surface of the polymer is easily scratched and exposure to abrasives will quickly produce an opaque haze. Blending it with other transparent engineering thermoplastics may improve some properties while maintaining its impact strength and transparency. Generally in a blend, miscibility is required for transparency.

Research has been performed in this area in recent years. Mondragon et al.<sup>2</sup> and Eguiazábal et al.<sup>3</sup> have blended polycarbonate with polyarylate. Both reported that a miscible blend forms but neither reported the mechanical properties of the blend. Robeson<sup>4</sup> suggests the miscibility that Mondragon et al.<sup>2</sup> and Eguiazábal et al.<sup>3</sup> found was due to ester-interchange reactions between the polycarbonate and the polyarylate. This would lead to the formation of a block copolymer of polycarbonate-polyarylate, which would act as a compatibilizer for the two polymers. Mondragon et al.<sup>2</sup> and Eguiazábal et al.<sup>3</sup> did not believe this to be the case.

Myers,<sup>5</sup> Myers and Brittain,<sup>6</sup> and Petersen et al.<sup>7</sup> blended polycarbonate with polysulfone. Petersen et al.<sup>7</sup> reported on a 1:1 mixture of the polymers in cyclohexanone solution; a film cast from the phase separated solution was not clear. These are signs that the polymers are immiscible. There are some difficulties with solution blending and casting of films. It is known that the choice of solvent is very critical. Two polymers may appear to be immiscible when cast from one solvent and are miscible when cast from another.<sup>8</sup> Also, polycarbonate, when cast from solution, has a tendency to crystallize.<sup>1</sup> Crystallization is a phase separating and purification mechanism to begin with, so any molecular mixing in solution is undone during the evaporation of the solvent. Myers and Brittain<sup>5,6</sup> reported that films of the blends cast from dichloromethane were immiscible. They also reprocessed the cast films by grinding them to a coarse powder and both compression molding and injection molding the powder. The compression molding would not be expected to further mixing. The type of injection molder that they used was a labo-

ratory benchtop device that was simply a transfer compression molder. First the material was heated to melt temperature in one chamber, then a ram forced the molten material through a die into a mold cavity. Under these conditions the amount of mixing was negligible. Due to the crystallization of the polycarbonate, it would be difficult for the material not to be heterogeneous. The viscosity of polymer solutions and the greater viscosity of polymer melts require a large expenditure of time and energy to insure an intimate mixture.

This work investigates the melt blending of polycarbonate with polysulfone and polyetherimide, and the resulting properties of the blends. Melt blending will insure that the polymers are intimately mixed. Since both polysulfone and polyetherimide have poorer impact properties compared to the polycarbonate, only compositions up to 20% polysulfone or polyetherimide will be examined.

## Experimental

### MATERIALS

The polycarbonates and the polyetherimide were obtained from the General Electric Company. The polycarbonates were natural transparent general purpose Lexan<sup>®</sup> 121, 141, and 161 with reported melt flow rates of 16.5, 9.5, and 8.0 g/10 min, respectively. The polyetherimide was natural transparent Ultem<sup>®</sup> 1000. Polyetherimide is a dark amber Bisphenol A-based transparent thermoplastic. It has outstanding chemical resistance<sup>9</sup> but poor impact strength. The polysulfone was obtained from Amoco Performance Products, Inc. and was the natural transparent general purpose grade Udel P-1700 with reported melt flow rate of 6.5 g/10 min. Polysulfone is a light amber Bisphenol A-based transparent thermoplastic.

### PROCESSING

#### Melt Blending

Polysulfone and polyetherimide pellets were weighed out to produce 5, 10, and 20% by weight blends, when mixed with Lexan<sup>®</sup> 161 polycarbonate. Twenty-four kilograms of polycarbonate pellets were placed into aluminum trays. The polysulfone or polyetherimide pellets for one blend

composition were added to the polycarbonate and mixed by hand until a visually uniform distribution was obtained. The mixture was then dried overnight at 125°C and then transferred to a drying hopper at 121°C. A Leistritz Laboratory Extruder LSM 3034 counter-rotating twin screw extruder with a low shear profile was used to blend the polymers. The material was extruded at 320°C with a screw speed of 105 rpm. A vacuum pump was connected at a vent zone of the extruder to pull off any additional moisture and low molecular weight material. The polymer was extruded into a water bath and then fed into a granulator where it was chopped into pellets and collected. The material processing rate was 3–5 kg/h. In addition to the 5, 10, and 20% polysulfone–polycarbonate and polyetherimide–polycarbonate blends, a blank of virgin polycarbonate was run to determine the effect of additional processing on the material.

### Injection Molding

Nine kilograms of polymer was dried for a minimum of 16 h at 125°C. Plaques 11.4 cm square by 3.2 and 1.6 mm thick were injection molded using a Van Dorn 200 injection molding machine. The maximum processing temperature, used for the polycarbonates and polycarbonate blends, was 330°C. For polysulfone, 360°C was the maximum processing temperature used for the 3.2 mm thick plaques and 400°C for the 1.6 mm thick plaques. The maximum processing temperature used for polyetherimide was 390°C. The mold temperature was set at 5°C below the glass transition temperature ( $T_g$ ), as determined by thermal analysis, of the polymer being molded. The polyetherimide could not be molded in the 1.6 mm thick cavity. Even operating under maximum injection pressure and barrel temperature, a short shot due to the long flow length and thinness of the plaque resulted.

## TESTING

### Differential Scanning Calorimetry

The thermal characterization to determine the glass transition temperatures was performed by using a DuPont 1090 Thermal Analyzer with a 910 differential scanning calorimeter (DSC) cellbase. Each material was cycled three times through its heating profile to eliminate the effects of its previous thermal history and to check for reproducibility. A scan rate of 5°C/min was used while purging with dry nitrogen at 40 mL/min. The poly-

carbonate was scanned from 30°C to 200°C, while the polysulfone, polyetherimide, and the blends were scanned from 30°C to 300°C.

### Thermal Dynamic Mechanical Analysis

The low temperature mechanical damping ( $\tan \delta$ ) behavior of the materials was examined by thermal dynamic mechanical analysis. Bars approximately 1.3 cm wide were machined from the 3.2 mm plaques. These bars were then tested on a DuPont 983 Dynamic Mechanical Analyzer controlled by a 2000 Thermal Analyzer from –150°C to the glass transition temperature of the sample for the pure polymers and the 20% blends and to 20°C for the 5 and 10% blends. A multiplexing–thermal step data acquisition program was used to analyze the samples. The frequencies used were 0.33, 1.0, 3.3, and 10 Hz with a temperature step interval of 2.5°C. Cooling of the sample and temperature control was accomplished by a DuPont LNCA-II liquid nitrogen cooling accessory.

A polynomial curve-fitting routine with up to 10 parameters was used to characterize the low temperature loss peak (gamma peak) of the polymers. The calculated curve was then used to determine the temperature of the peak maximum and a normalized peak area. The peak area was determined by integrating the calculated curve and subtracting the area below the baseline. The area was normalized by dividing the area by the width of the temperature limits of the integration. This procedure shifts the result to emphasize the magnitude of the peak, rather than the area of broadness. Activation energies for the polymers were determined from a plot of  $\ln(\text{frequency})$  versus the reciprocal absolute temperature of the peak maximum. The slope of this line, multiplied by the gas constant  $R$ , yielded the activation energy shown in the following equation<sup>10</sup>:

$$\frac{1}{f} = Ae^{-Ea/RT} \quad (1)$$

where  $f$  = the frequency of the test;  $Ea$  = the activation energy;  $R$  = the gas constant;  $T$  = the absolute temperature; and  $A$  = the preexponential constant.

### Impact Testing

Impact strength was determined by using Izod and Charpy pendulum impact testing. Izod and

Charpy bars were cut from the 3.2 mm thick molded plaques and separated into two sets: bars cut either transverse or longitudinal to the flow direction. Each sample set contained between 10 and 18 samples. The bars were machined to size, notched, and tested with a TMI pendulum impact machine according to ASTM D256-84 Standard Test Method for Impact Resistance of Plastics and Electrical Insulating Materials.<sup>11</sup> The one exception from the standard test was that the bars for Charpy impact were only 11.4 cm long instead of the standard minimum of 12.7 cm due to the size of the mold cavity.

### Tensile Testing

The yield and break stresses and elongations were determined using an Instron mechanical testing machine. The values for the raw data of yield and break load and elongation were determined by a Microcon I computer attached to the testing machine. Type V microtensile bars were cut from the molded plaques of both thicknesses and separated into two sets: bars cut either transverse or longitudinal to the flow direction. The bars were machined to size and tested at 1.27 and 127 mm/min strain rate according to ASTM D638-87 Standard Test Methods for Tensile Properties of Plastics.<sup>12</sup> Each sample set contained 10 samples, 5 for each rate of testing.

### Ballistic Testing

The ballistic performance was evaluated by testing the plaques according to MIL-STD-662E V<sub>50</sub>

Ballistic Test for Armor<sup>13</sup> using a high-pressure helium gas gun. A 17-grain fragment simulator was used as the projectile. The test plaques were rigidly held in a sample holder made from two 33 cm square, 1.9 cm thick aluminum plates bolted together and placed in a mount. Four 2.5 cm diameter holes in the plates located in the center of each corner quadrant provided for the passage of the projectile through the plaques. After each shot, the sample holder was rotated in its mount to align the next sample. After a set of four shots, the holder was removed from the mount, opened, and the samples repositioned for the next shots. A schematic of the test setup is shown in Figure 1.

Four light screens were used as triggers for timers to record the time-of-flight of the projectile to determine the velocity of the projectile before and after impact. The timers recorded the time-of-flight between screens 1 & 2, 2 & 3, 3 & 4, and 1 & 4 as a check. Measuring the distances between each of the screens and target, and the time-of-flight between screens 1 & 2, and between 3 & 4, the velocities at the midpoint between each set of screens can be determined. The distances from the midpoint of screens 1 & 2, and of 3 & 4, to the target are referred to as S1 and S2, respectively. The striking and residual velocities were determined by taking the air resistance into account over S1 and S2 as shown in eqs. (2) and (3) below<sup>14</sup>:

$$V_s = V_{12} \left( 1 - \frac{S1}{C} \right) \quad (2)$$

$$V_r = V_{34} \left( 1 - \frac{S2}{C} \right) \quad (3)$$

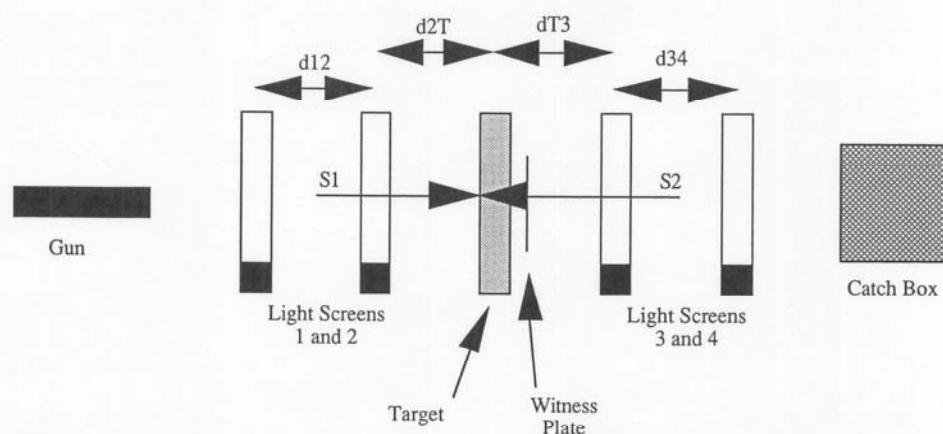


FIGURE 1. Diagram of ballistic test setup.

where  $V_s$  = the striking velocity of the projectile;  $V_{12}$  = the velocity at the midpoint between screens 1 & 2;  $S_1$  = the distance from midpoint between screens 1 & 2 and the target;  $C$  = correction constant, 52.4 m;  $V_r$  = the residual velocity after penetration;  $V_{34}$  = the velocity at the midpoint between screens 3 & 4; and  $S_2$  = the distance from midpoint between screens 3 & 4 and the target.

A 0.05 mm thick aluminum witness plate was used to record complete penetrations. A complete penetration is defined as occurring when the impacting projectile, or any fragment thereof, or any fragment of the test specimen perforates the witness plate, resulting in a crack or hole that permits the passage of light when a 60-watt, 110-volt bulb is placed proximate to the witness plate.<sup>13</sup> A catch box, layered with felt pads and Kevlar<sup>®</sup> fabric, was used to stop the projectile.

Two different characteristic velocities,  $V_{50}$  and  $V_c$ , were calculated.  $V_{50}$ , the velocity at which 50% of the impacts result in complete penetration, was calculated from the arithmetic mean of the five highest partial and five lowest complete penetration impact velocities.  $V_c$ , the critical velocity for complete penetration, was calculated by fitting the following equations to a plot of all striking velocities greater than and equal to the lowest complete penetration velocity versus the residual velocities<sup>15,16</sup>:

$$V_r^2 = A V_s^2 - B \quad (4)$$

$$V_c^2 = \frac{B}{A} \quad (5)$$

$$V_r = (A(V_s^2 - V_c^2))^{1/2} \quad (6)$$

where  $V_s$  = the striking velocity of the projectile;  $V_r$  = the residual velocity after penetration;  $V_c$  = the critical velocity for complete penetration;  $A$  = the slope of the line; and  $B$  = the intercept. A minimum of 32 shots was used for each set of samples, with at least eight shots spread over the range from  $V_{50}$  to approximately 120 m/s above the  $V_{50}$ . While the  $V_{50}$  is simply a statistical mean, the  $V_c$  is more a measurement of the kinetic energy required to completely penetrate the sample for a projectile of a given size and mass. In either case, the  $V_{50}$  and the  $V_c$  will increase for tougher samples requiring a greater impact energy for penetration.

## Results and Discussion

### PROCESSING

The visible appearance of the polycarbonate-polysulfone blends was white in color ranging from translucent to opaque with increasing concentration of polysulfone. The polycarbonate-polyetherimide blends ranged from beige to a light tan in color with increasing concentration of polyetherimide and were opaque. The polycarbonate blank was darker in color, without the characteristic blue tint. The visual appearance of the blends was very homogeneous. No phase separation was visible to the naked eye. However, the mixing of two transparent materials yielding a translucent or opaque material would suggest a two phase system separated on a microscopic scale.

The 3.2 mm thick molded plaques of the polycarbonates appeared as normal polycarbonate possessing the characteristic bluish coloring when seen from the side. The 1.6 mm plaques were very different in coloring from one another. The Lexan<sup>®</sup> 121 lacked the bluish coloring but otherwise appeared normal. The Lexan<sup>®</sup> 141 had a pale orange tint that was very noticeable when viewed from the side. The Lexan<sup>®</sup> 161 also lacked the bluish coloring but appeared grayish when viewed from the side. The injection molded plaques indicate that the polycarbonates have undergone slight color changes. These color changes are important because they reflect chemical changes in the polymer system. Causes for the differences in coloration between the plaques of different thickness as well as different materials may be traced to barrel temperature and injection or "boost" pressure. The 1.6 mm thick Lexan<sup>®</sup> 121 plaques were processed at the same temperature as the 3.2 mm plaques but at a much higher injection pressure. The 1.6 mm thick Lexan<sup>®</sup> 141 and 161 plaques were molded at both a higher temperature and higher injection pressure than the 3.2 mm plaques to fill the thinner cavity. The shot size for the thinner plaques was 30% smaller than for the thicker plaques. This difference results in the material experiencing a 30% longer residence time in the barrel of the injection molder at a higher temperature. The higher injection pressure and thinner section cause greater shear forces in the material. These conditions could lead to material degradation resulting in discoloration and/or reduction in mate-

## POLYCARBONATE BLENDS

rial properties. The polysulfone and polyetherimide plaques appeared normal with no discoloration or any other visible defects.

Plaques molded from the polycarbonate-polysulfone blends were tan in color. The thinner plaques were translucent while the thicker ones were opaque. Plaques molded from the polycarbonate-polyetherimide blends ranged from beige to a dark tan in color with increasing concentration of polyetherimide and were opaque. The plaques molded from the extruded polycarbonate blank were light amber in color, greatly resembling natural polysulfone.

### TESTING

#### Differential Scanning Calorimetry

Table I summarizes the results of the DSC characterization of the neat polymers and blends. The presence of two  $T_g$ s in the blends, with little if any shifting from where they would normally occur in each of the resins, indicates that the polycarbonate-polysulfone and polycarbonate-polyetherimide blends are immiscible.<sup>17</sup>

#### Thermal Dynamic Mechanical Analysis

Representative thermograms for the mechanical damping of polycarbonate, polysulfone, and

polyetherimide are shown in Figure 2. Thermograms for the blends are very similar to the thermograms for polycarbonate, which is not surprising since polycarbonate is the major component in all cases. The peak maxima and activation energies from the 983 DMA data are listed in Table II. The normalized peak areas are listed in Table III. The activation energy for the polymers and the blends is basically the same within the precision of the experiment except for polyetherimide, which is lower than the rest. The bisphenol A repeat unit is the major common feature between the polymers and since it is the major energy absorbing feature in the polymers, it is not surprising that the activation energy is similar.

Upon examining the data from the peak area calculation, it was found that a plot of the peak area versus  $\log(\text{frequency})$ , shown in Figures 3 and 4, yielded a linear fit with a correlation coefficient of 0.969 or better for all materials. The slope of these lines ranged from  $1.2 \times 10^{-3}$  to  $1.9 \times 10^{-3}$  for the polycarbonates and the blends,  $1.1 \times 10^{-3}$  for polysulfone, and  $-3.5 \times 10^{-4}$  for polyetherimide. Figure 4 shows a similar behavior for the polyetherimide blends. The peak area drops in magnitude from that of the polycarbonate to a level slightly lower than the polysulfone blends. The slopes of the lines for the polyetherimide blends are also equivalent to the polycarbonate line.

The magnitude of the peak area is an indication

**TABLE I**  
Glass Transition Temperatures of Polymers and Blends Measured by Differential Scanning Calorimetry

Material	$T_g$ (°C) due to PC	$T_g$ (°C) due to PSU or PEI
Lexan® 121	146	n/a
Lexan® 141	147	n/a
Lexan® 161	147	n/a
Processed Lexan® 161	146	n/a
Polysulfone (PSU)	n/a	186
Polyetherimide (PEI)	n/a	216
5% PSU/Lexan® 161 blend	146	187
10% PSU/Lexan® 161 blend	147	184
20% PSU/Lexan® 161 blend	145	186
5% PEI/Lexan® 161 blend	146	216
10% PEI/Lexan® 161 blend	148	216
20% PEI/Lexan® 161 blend	145	212

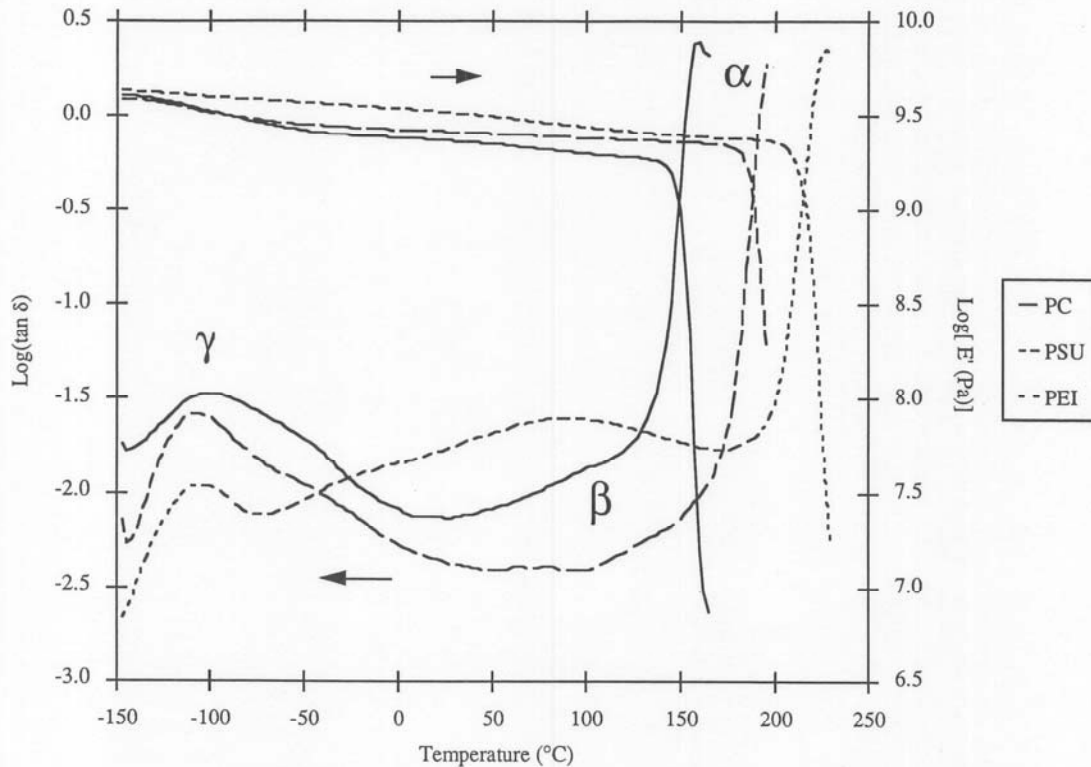


**FIGURE 2.** Mechanical damping and storage modulus thermogram of polycarbonate, polysulfone, and polyetherimide. Alpha, beta, and gamma transitions are shown.

**TABLE II**  
Gamma Peak Temperatures and Activation Energy of Polymers and Blends

Material	Peak Temperatures (°C)				Activation Energy (kJ/mol)
	0.33 Hz	1.0 Hz	3.3 Hz	10. Hz	
Lexan® 121	-102.0	-97.0	-90.9	-84.7	53
Lexan® 141	-105.1	-100.0	-93.5	-86.9	49
Lexan® 161	-104.0	-98.9	-92.5	-86.3	50
Processed Lexan® 161	-104.4	-99.1	-92.9	-86.9	51
Polysulfone (PSU)	-112.5	-107.4	-101.7	-95.7	48
Polyetherimide (PEI)	-114.1	-108.7	-102.0	-95.8	43
5% PSU/Lexan® 161 blend	-105.9	-101.4	-94.6	-88.1	49
10% PSU/Lexan® 161 blend	-105.7	-101.2	-94.5	-88.5	50
20% PSU/Lexan® 161 blend	-106.7	-101.8	-95.3	-89.0	49
5% PEI/Lexan® 161 blend	-105.2	-100.4	-94.1	-87.6	50
10% PEI/Lexan® 161 blend	-106.6	-101.4	-94.8	-88.2	47
20% PEI/Lexan® 161 blend	-106.2	-101.2	-94.7	-88.2	48

**TABLE III**  
Normalized Gamma Peak Areas of Polymers and Blends

Material	Normalized Gamma Peak Areas $\times 10^3$			
	0.33 Hz	1.0 Hz	3.3 Hz	10. Hz
Lexan® 121	7.73	8.08	8.59	10.18
Lexan® 141	8.94	9.76	10.65	11.23
Lexan® 161	9.24	10.01	11.21	12.01
Processed Lexan® 161	9.26	9.68	10.64	11.67
Polysulfone (PSU)	8.36	8.83	9.13	10.04
Polyetherimide (PEI)	3.11	3.04	2.85	2.59
5% PSU/Lexan® 161 blend	7.90	8.80	9.70	10.44
10% PSU/Lexan® 161 blend	8.05	8.61	9.37	10.22
20% PSU/Lexan® 161 blend	8.24	8.80	9.47	10.25
5% PEI/Lexan® 161 blend	7.38	8.12	9.08	10.18
10% PEI/Lexan® 161 blend	6.41	7.03	7.63	8.35
20% PEI/Lexan® 161 blend	6.95	7.39	8.09	8.79

of the material constituent of the sample. The polycarbonates with the higher melt viscosity had larger peak areas. For the polysulfone blends, as seen in Figure 3, the magnitude of the peak area is at the same level as for the polysulfone and the slopes of the lines are equivalent to the polycarbonate line. The size of the low temperature loss

peak is believed to correlate to the toughness of the material.<sup>18</sup> The peak area size increases linearly with log (frequency), which suggests that the material absorbs and dissipates more energy at higher frequencies over the temperature range. The similar slope for the blends and polycarbonate is expected since the blends are primarily polycarbo-

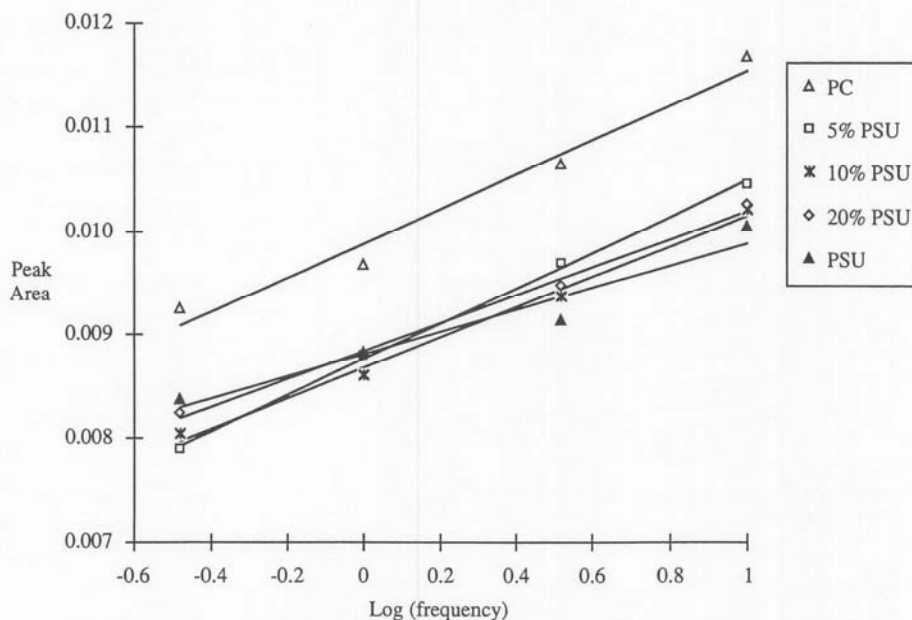


**FIGURE 3.** Gamma peak area versus log(frequency) of polysulfone blends.

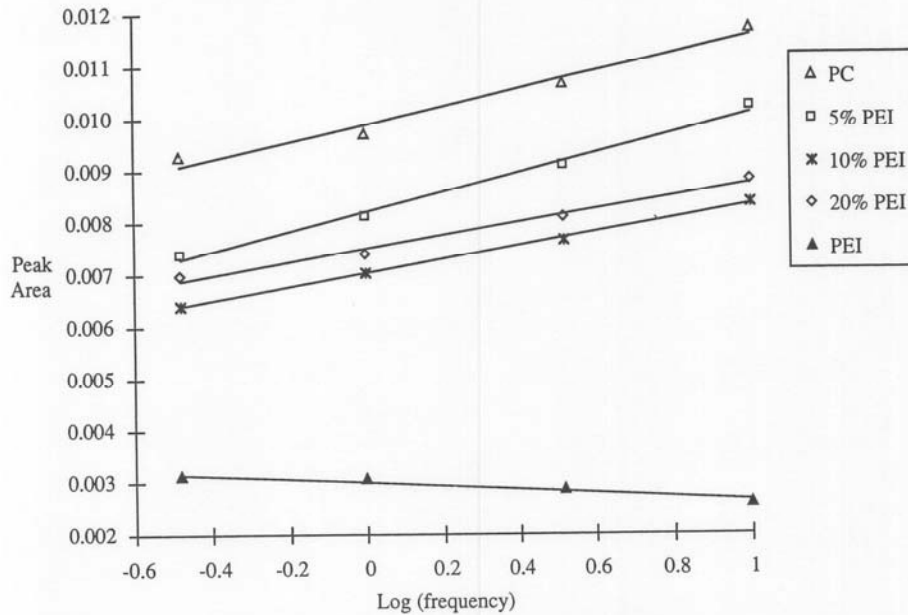


FIGURE 4. Gamma peak area versus log(frequency) of polyetherimide blends.

nate. With only a maximum of 20% polysulfone and phase separated, the material is likely to be a polycarbonate matrix filled with polysulfone particles. The slope of the line of normalized peak area versus log(frequency) reflects the polycarbonate matrix while the magnitude of the normalized peak area reflects the difference between neat and blended polycarbonate. The values of the normalized peak area for the polycarbonate-polysulfone blends and polysulfone are all quite close together and no significant difference or trends can be determined.

Figure 4 shows a similar behavior for the polyetherimide blends. The peak area drops in magnitude from that of the polycarbonate to a level slightly lower than the polysulfone blends. The slope of the lines for the polyetherimide blends are also equivalent to the polycarbonate line. The peak areas for the polyetherimide sample are much smaller than for the polycarbonates, polysulfone, and the blends. The slope of the line of normalized peak area versus log(frequency) for the polyetherimide is negative, which suggests that the material absorbs and dissipates less energy at higher frequencies over the temperature range. This may explain why the polyetherimide behaves in a ductile manner in tensile tests with low strain rates but fails in a brittle manner in high strain rate impact tests.

### Impact Testing

Many of the sample sets had specimens that fractured by a different failure mechanism than the majority of the specimens in that sample set. The minority or secondary failure mechanism is considered a deviation or departure from the norm. These differences manifest themselves in the mode of failure (ductile or brittle) and impact strength. A bimodal distribution occurs with impact strengths of approximately 190 J/m of notch for brittle fracture and 850 J/m of notch for ductile fracture. Graphs of the impact strength of the polymer blends that fractured by the primary failure mechanism for that data set versus the percent composition are shown in Figures 5 and 6 for the Izod and Charpy tests. As seen in Figure 5, the polysulfone blend samples show a change in impact strength at 10% loading. Half of the sample sets at 10% polysulfone reflect a lower impact strength and a brittle failure mechanism. At 20% polysulfone, only the Charpy sample set cut longitudinally to the flow direction still maintains high impact strength. Figure 6 shows that the polyetherimide blends exhibit a large drop in the impact strength with polyetherimide levels of 20%.

There is little variation in the impact strength for ductile failure or for brittle failure, respectively. A greater understanding of the material behavior can

## POLYCARBONATE BLENDS

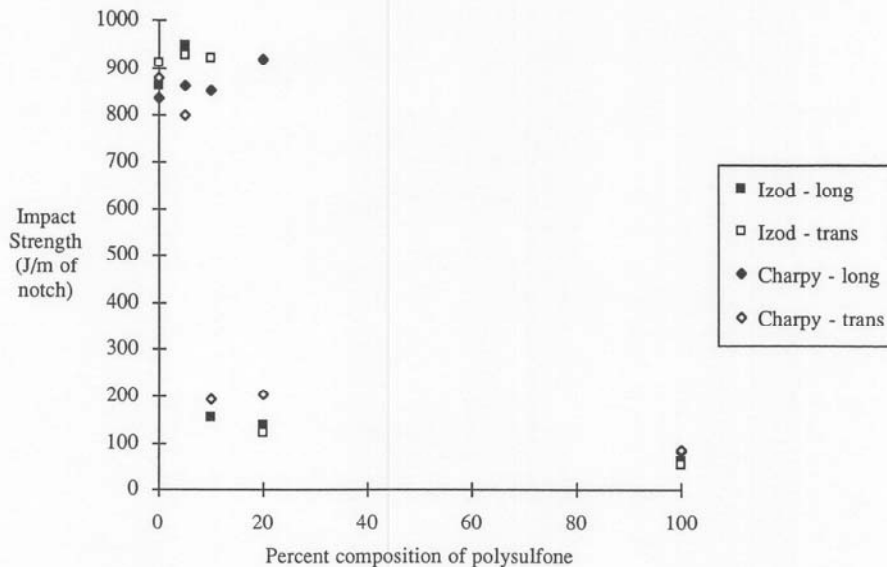


FIGURE 5. Impact strength versus percent composition of polysulfone blends.

be gained from Figures 7 and 8, which show the percent distribution of failure type within a sample set. These graphs reflect with greater clarity the changes in impact behavior with varying composition. The polysulfone blend shows a significant decrease in ductile failures with 5% polysulfone. Increasing polysulfone concentration causes even fewer ductile failures, with the plot in Figure 7 resembling a decay curve. The behavior of the polyetherimide blends shown in Figure 8 reveals a

high level of ductile failure, up to 10% polyetherimide. At 20% polyetherimide, there is a sharp drop in the number of ductile failures.

This drop in the percentage of ductile failures is obviously caused by the increase in composition of the brittle component. How is the change in composition affecting the material to change the overall impact properties? If the blends were miscible but without interaction between the polymers, one would expect the material to behave according to a

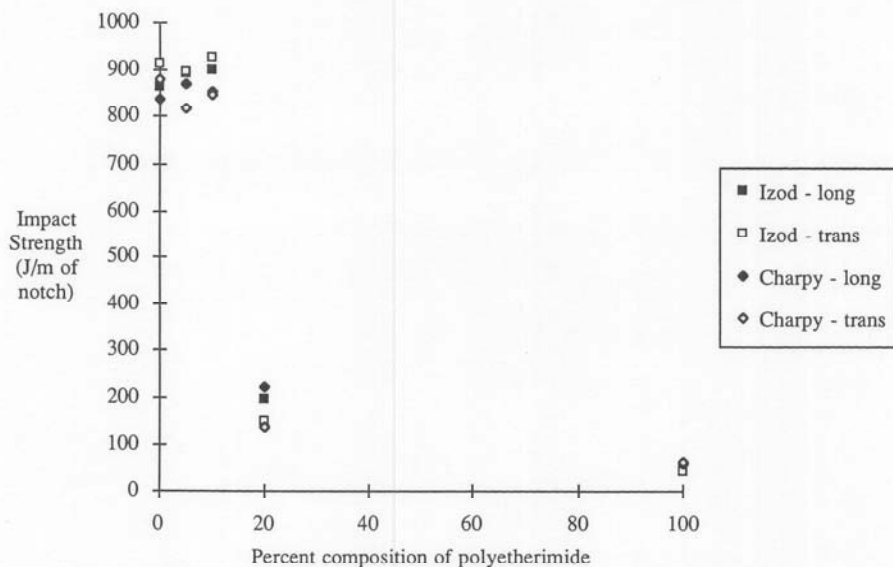


FIGURE 6. Impact strength versus percent composition of polyetherimide blends.

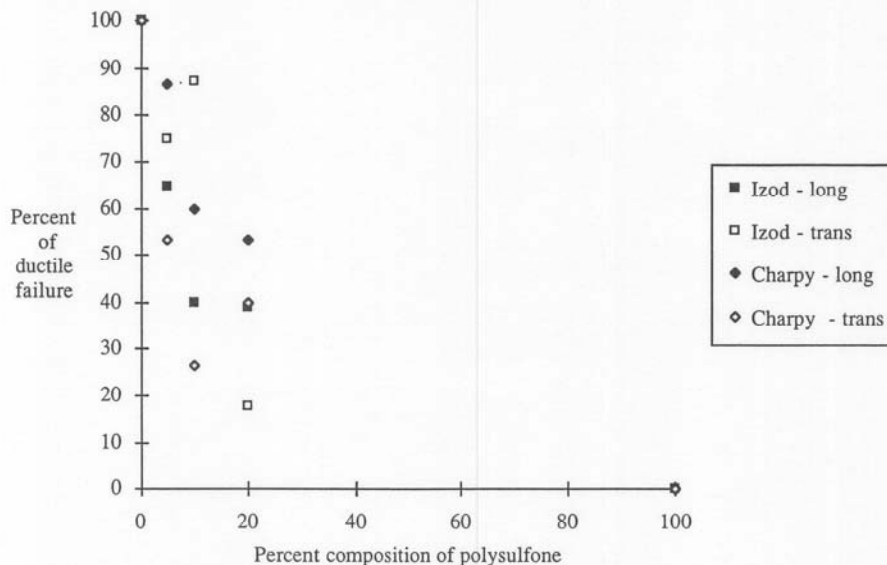


FIGURE 7. Percent of ductile failure versus percent composition of polysulfone blends.

rule of mixtures.<sup>19,20</sup> This would have manifested itself in either a linear or slightly curved decrease in impact strength or percentage of ductile failures with increasing composition of the brittle polymer. With an immiscible system, the resulting properties can be further divided between semicompatible and incompatible. In an incompatible system, the property in question drops quickly with only a small addition of the other component to a value that is below either component. In a semicompatible system, the property in question remains un-

changed until the percentage of the second component reaches a certain level. The property then changes to that of the second component where it remains unchanged for the remaining compositions. This transition occurs over a small compositional range of 5–10%. This transition is attributed to a morphological change in the material. As the concentration of the dispersed phase increases, its morphology can change from spheres to cylinders to lamellae to finally a continuous phase.<sup>21</sup> While there is no direct proof, an easy explanation for a

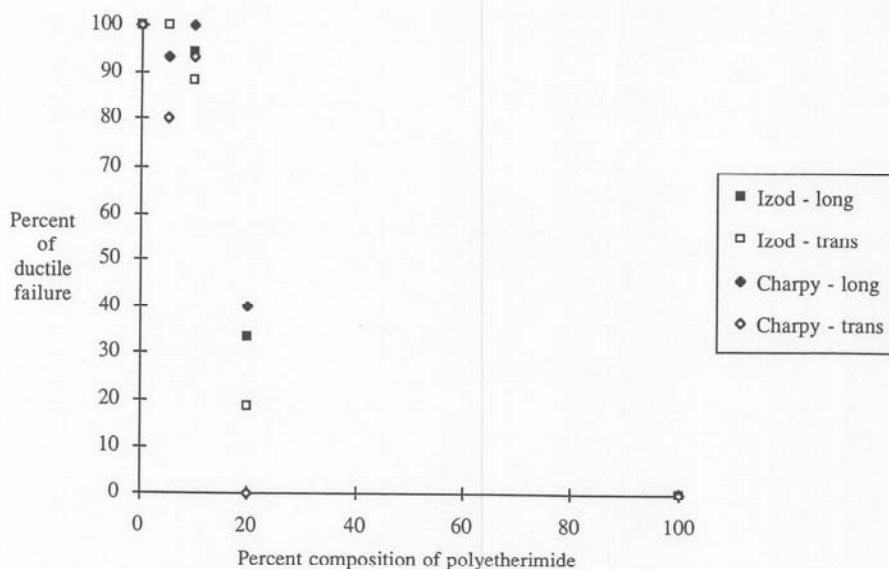
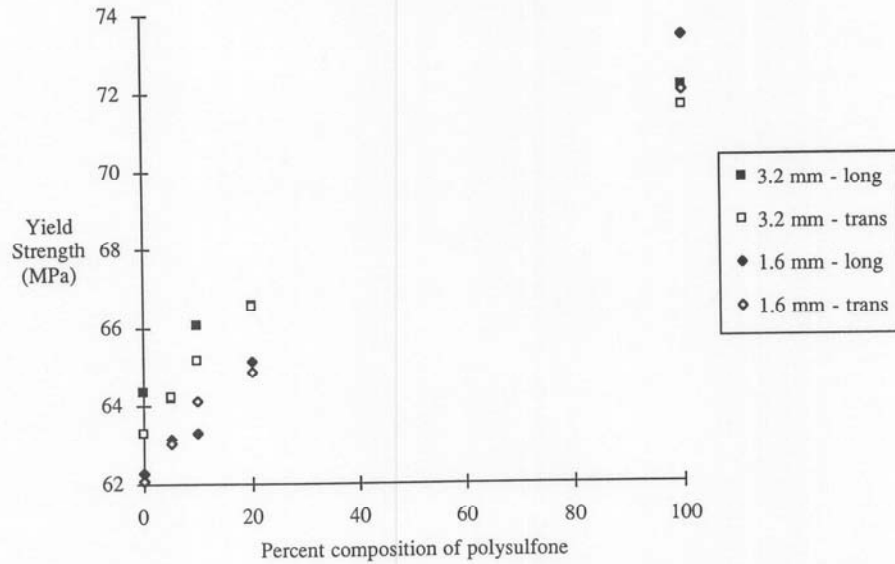


FIGURE 8. Percent of ductile failure versus percent composition of polyetherimide blends.

## POLYCARBONATE BLENDS



**FIGURE 9.** Yield strength versus percent composition of polysulfone blends at 1.27 mm/min strain rate.

ductile to brittle transition is a morphological change that forms connected brittle phase domains across the test sample allowing the crack to propagate through the brittle phase.

The difference in behavior between the two sets of blends may indicate interaction between the polycarbonate and the polysulfone. The high number of ductile failures for the 5 and 10% polycarbonate-polyetherimide blend may show that the polyetherimide is acting as an inert filler. The rapid drop in the number of ductile failures with increasing concentration for the polycarbonate-poly-

sulfone blends may indicate that the polysulfone is imparting the brittle nature of its failure mechanism at a lower concentration than for the polycarbonate-polyetherimide through interaction with the polycarbonate.

### Tensile Testing

The tensile testing examined the yield strength and elongation for the polymers, while investigating the effects of the sample orientation to the flow direction, the thickness of the sample, which cor-

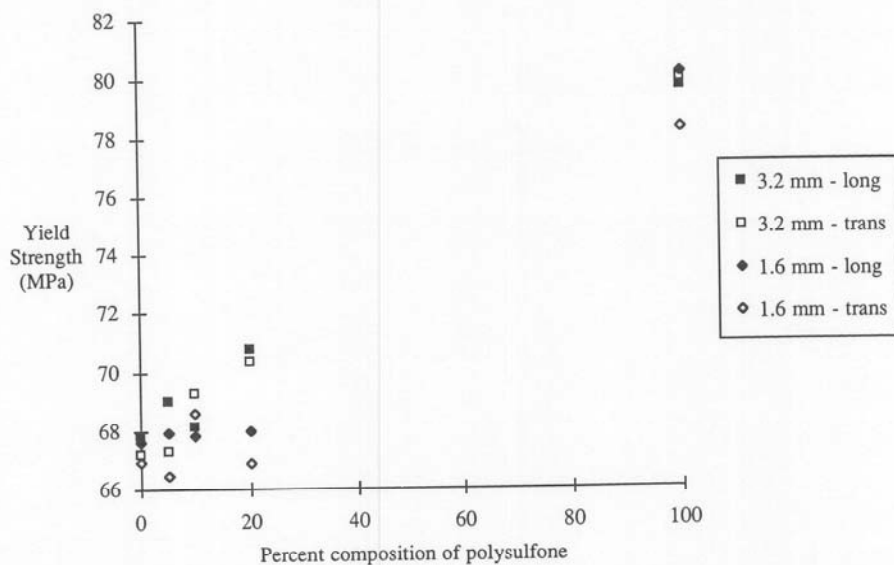


**FIGURE 10.** Yield strength versus percent composition of polysulfone blends at 127 mm/min strain rate.

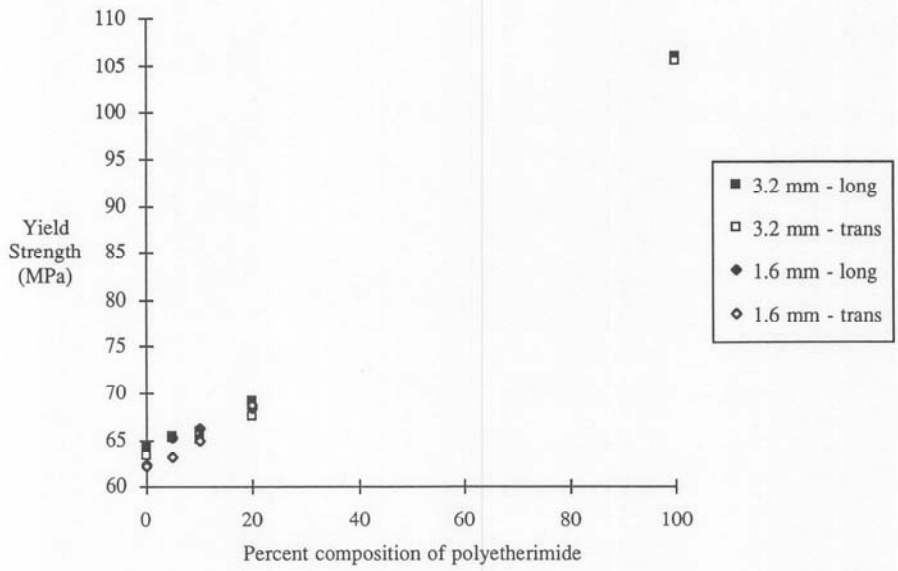


FIGURE 11. Yield strength versus percent composition of polyetherimide blends at 1.27 mm/min strain rate.

responds to different levels of shear stress during molding, the rate at which the test was performed, and the different materials. The graphs of the results for the yield strength of the blends in Figures 9–12 can explain some of the behavior of the blends. The thicker samples had a consistently higher yield strength for the 1.27 mm/min strain rate; however, this relationship does not hold completely true for the 127 mm/min strain rate samples. The average values of the yield strength for

the 127 mm/min strain rate were consistently 3.4–4.1 MPa greater than for the 1.27 mm/min strain rate.

Taking the results for the yield strength versus percent composition for a given strain rate as a whole, it is clear that the yield strength increases with increasing composition of polysulfone or polyetherimide if an average value is used for each composition. This increase appears to be linear but an extrapolation to 100% polysulfone or poly-

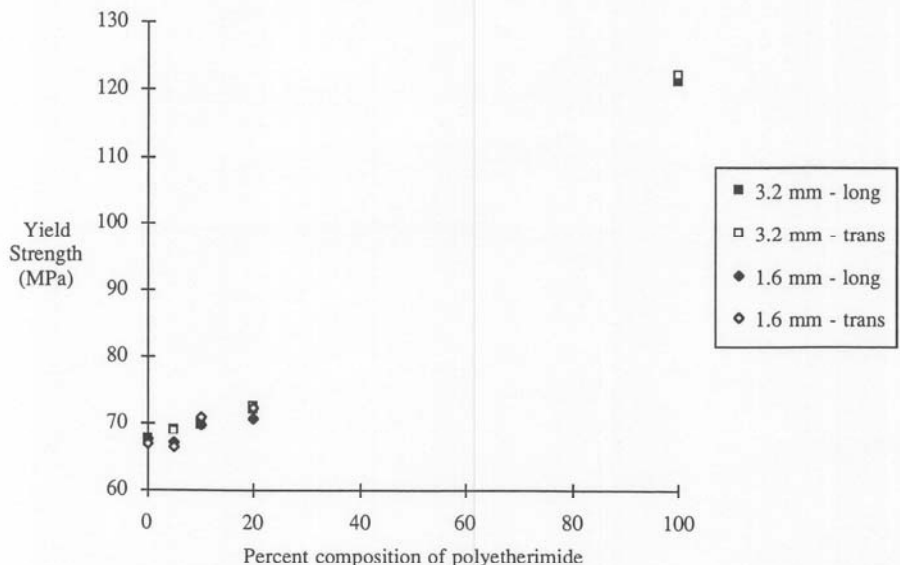


FIGURE 12. Yield strength versus percent composition of polyetherimide blends at 127 mm/min strain rate.

**TABLE IV**  
 **$V_{50}$  and  $V_c$  for 3.2 and 1.6 mm Thick Polymers and Blends**

Material	$V_{50}$ (3.2 mm) (m/s)	$V_c$ (3.2 mm) (m/s)	$V_{50}$ (1.6 mm) (m/s)	$V_c$ (1.6 mm) (m/s)
Lexan® 121	230	231	141	137
Lexan® 141	221	221	133	136
Lexan® 161	218	221	130	136
Processed Lexan® 161	215	218	139	136
Polysulfone (PSU)	202	204	132	137
Polyetherimide (PEI)	106	109	na	na
5% PSU/Lexan® 161 blend	225	224	137	136
10% PSU/Lexan® 161 blend	220	221	136	134
20% PSU/Lexan® 161 blend	219	220	133	135
5% PEI/Lexan® 161 blend	225	226	138	139
10% PEI/Lexan® 161 blend	217	219	134	134
20% PEI/Lexan® 161 blend	212	213	123	121

etherimide underestimates the measured value except for the polysulfone blends at 1.27 mm/min strain rate, which overestimates the measured value. This indicates that a line describing the yield strength versus percent composition across the entire compositional range would either be curved or discontinuous. The amount of change in yield strength for a given change in composition is much greater in the polyetherimide blends, which is not

surprising since polyetherimide has a much greater yield strength than polysulfone.

### Ballistic Testing

Table IV lists the calculated  $V_{50}$  and  $V_c$  for the 3.2 and 1.6 mm thick plaques of the neat and blended polymers. Graphs of the material composition versus  $V_c$  are shown in Figures 13 and 14. In addition

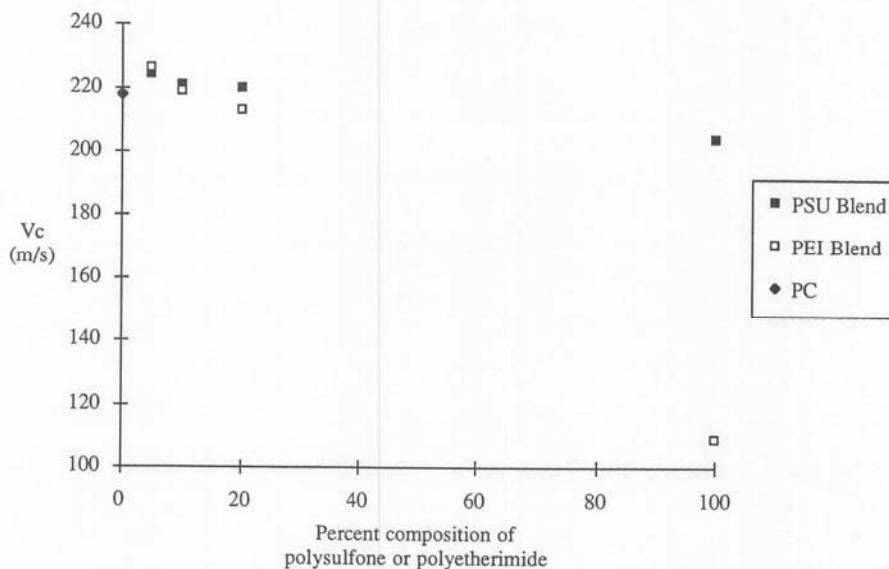


**FIGURE 13.** Critical velocity versus composition of 3.2 mm plaques.

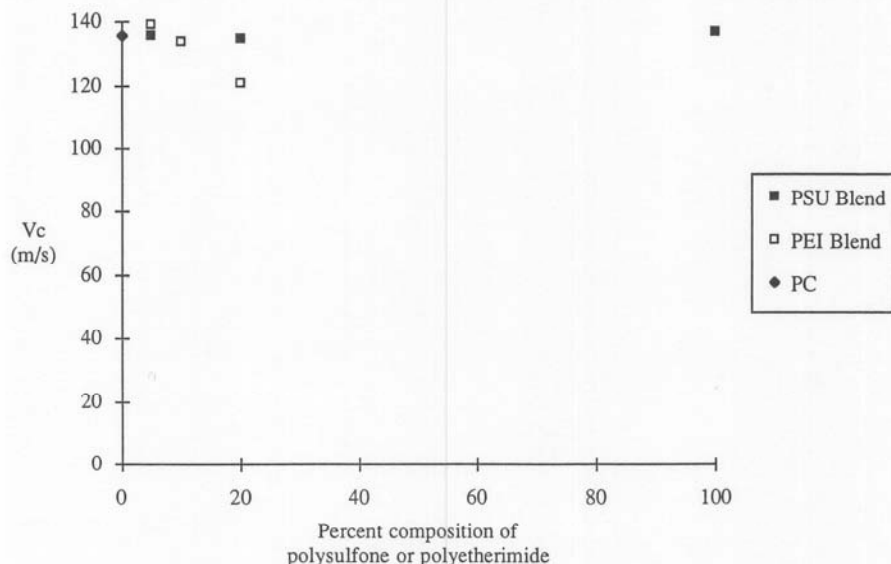


FIGURE 14. Critical velocity versus composition of 1.6 mm plaques.

to the  $V_c$  and  $V_{50}$ , the failure mechanism is an important consideration. The desired failure mechanisms are punching or petalling, which are of a ductile nature. Spalling, whether it is delamination of a rear section or a blowout of a section larger than the impact area, is undesirable. Sharp edges and high velocities of spall can cause damage to body tissues. The MIL-STD-662E  $V_{50}$  Ballistic Test for Armor<sup>13</sup> requires the use of a 0.002 in. thick aluminum witness plate to record complete penetrations. The projectile may actually be stopped by the material but if a fragment or spall punctures the witness plate, the penetration is considered complete.

The Lexan<sup>®</sup> 121 was prone to brittle failure resulting in a large amount of spalling and cracking. The Lexan<sup>®</sup> 141 and 161 by contrast had only one brittle failure and some minor cracking that could be related to previous tests or visible defects located near the point of impact. This difference in the failure mechanism led to the rejection of Lexan<sup>®</sup> 121 to blend with the polysulfone and polyetherimide even though its  $V_c$  was 10 m/s greater for the 3.2 mm plaques than the other polycarbonates. The difference in  $V_c$  for the 1.6 mm plaques of the polycarbonates is insignificant. The Lexan<sup>®</sup> 161 was chosen over the Lexan<sup>®</sup> 141 because there was concern at that time that the repeated processing of the polymer by blending and molding could reduce the molecular weight and lead to a reduction in physical properties. Since there was no difference in the  $V_c$  and insignificant

difference in the  $V_{50}$  between the materials, it was decided to use the higher molecular weight material. The testing of the polysulfone plaques resulted in a significant number of impacts causing spalling or cracking in the samples. With the polyetherimide samples, every impact caused radial cracking and spalling.

In Figure 13, it can clearly be seen that in the 3.2 mm thick samples, an initial increase in  $V_c$  occurs at 5% of either polysulfone or polyetherimide in the blend composition. However, this increase may not be statistically significant. It is then followed by what appears to be a linear decrease in  $V_c$  with increasing loading of polysulfone or polyetherimide. The same results are found in the 1.6 mm thick samples for polyetherimide. The values of the  $V_c$  for 1.6 mm thick polycarbonate and polysulfone are almost the same and the  $V_c$  of the polysulfone blends are scattered about those values.

The 3.2 mm thick processed polycarbonate plaques had only one impact that caused cracking and the 1.6 mm thick plaques had a few impacts that appeared to tear the material rather than to crack it. The polycarbonate-polysulfone blends showed general increasing brittleness, with increasing concentration of polysulfone. The 5% blend behaved in a similar manner to the processed polycarbonate. The 10% blend had increased cracking and an incident of spalling in each thickness. The 3.2 mm thick plaques of the 20% polycarbonate-polysulfone showed about the same amount of cracking as the 10% blend, but the

cracking appeared to be less severe and there were no cases of spalling. The 1.6 mm thick plaques actually went against the trend with no brittle failures; so overall they were more ductile. The polycarbonate-polyetherimide blends showed increasing brittleness that resulted in additional cracking and spalling with increasing polyetherimide concentration. In general terms, there are only slight differences between each set of blends.

An interesting finding is uncovered when the ballistic results are compared to the pendulum impact results. The polysulfone failed in a brittle manner for all of the Izod and Charpy impact tests but in ballistic tests the polysulfone failed in a ductile manner. This seems to be counter-intuitive, that the pendulum test with a velocity of impact of 3.5 m/s would produce brittle failures and the ballistic test with impact velocities of 100 to 300 m/s would produce ductile failures. Since the pendulum test samples were notched, this result may be displaying the notch-sensitivity of polysulfone and not its response to the speed of impact.<sup>22</sup> This effect may also explain the greater percentage of brittle failures in the pendulum impact tests than in the ballistic tests for the polycarbonate-polysulfone blends.

## Conclusions

The extrusion of the blends and the subsequent molding of the blend demonstrates the processability of the blends. It is obvious from the DSC results and visible appearance that the blends of polycarbonate with polysulfone and polyetherimide are immiscible. The effect of the repeated processing of the polymers did affect the appearance of the polymers by a discoloration of the polycarbonate.

From the DMA data analysis, a linear relationship exists between the normalized  $\gamma$  loss peak area and the  $\log(\text{frequency})$ . For polycarbonate, polysulfone, and all compositions of the polycarbonate-polysulfone and polycarbonate-polyetherimide blends, the relationship is positive. For polyetherimide the relationship is slightly negative. The activation energy for each of the materials was approximately 50 kJ/mol.

The tensile test results indicate that a possible linear relationship exists between the percent composition and the yield strength for the blends. The

tensile data of the blends actually show an improvement in tensile strength.

The ballistic testing results show that a possible linear relationship exists between the percent composition and the  $V_c$ . The calculations of  $V_c$  and  $V_{50}$  are performed in very different ways but result in values that are quite similar for the same samples. The lack of transparency precludes the use of the blends for many of the applications for which polycarbonate is best suited; however, both sets of the blends exhibit good to fair ballistic impact properties up to at least 20% polysulfone or polyetherimide.

The Izod and Charpy impact test data reveal a bimodal distribution of impact strength for the blends. The average impact strength and percentage of ductile failures decrease with increasing composition of polysulfone and polyetherimide. The difference between the brittle failure mechanism displayed in the pendulum impact samples and the ductile failure mechanism displayed in the ballistic impact samples for the polysulfone is a manifestation of the notch-sensitivity of polysulfone. When comparing the pendulum impact results for the two sets of blends, this effect reveals an interaction between polycarbonate and polysulfone by a greater percentage of brittle failures in the polycarbonate-polysulfone blends than in the polycarbonate-polyetherimide. This is particularly shown in the 5 and 10% blends.

## References

1. K. J. Saunders, *Organic Polymer Chemistry*, 2nd Ed., Chapman and Hall, New York, 1988, pp. 272-274.
2. I. Mondragon, M. M. Cortázar, and G. M. Guzmán, *Makromol. Chem.*, **184**, 1741 (1983).
3. J. I. Eguiazábal, M. E. Calahorra, M. M. Cortázar, and J. J. Iruin, *Polym. Eng. Sci.*, **24**, 608 (1984).
4. L. M. Robeson, *J. Appl. Polym. Chem.*, **30**, 4081 (1984).
5. F. S. Myers, "Properties and Microstructure of Polycarbonate-Polysulfone Blends." Ph.D. dissertation, Northwestern University, 1971.
6. F. S. Myers and J. O. Brittain, *J. Appl. Polym. Sci.*, **17**, 2715 (1973).
7. R. J. Petersen, R. D. Corneliussen, and L. T. Rozelle, *Polym. Prepr.*, **10**, 385 (1969).
8. M. Bank, J. Leffingwell, and C. Thies, *Macromolecules*, **4**, 43 (1971).
9. K. J. Saunders, *Organic Polymer Chemistry*, 2nd Ed., Chapman and Hall, New York, 1988, pp. 220-221.

10. L. E. Nielsen, *Mechanical Properties of Polymers*, Reinhold Publishing Corp., New York, 1962, p. 161.
11. ASTM D256-84, "Standard Test Methods for Impact Resistance of Plastics and Electrical Insulating Materials." *Annual Book of ASTM Standards*, Vol. 08.01.
12. ASTM D638-87, "Standard Test Methods for Tensile Properties of Plastics." *Annual Book of ASTM Standards*, Vol. 08.01.
13. Military Standard, MIL-STD-662E, 22 January 1987, "V<sub>50</sub> Ballistic Test for Armor."
14. R. A. Muldoon, *Watertown Arsenal Laboratory Report No. WAL 760/503*, 27 January 1953.
15. R. F. Recht and T. W. Ipson, *J. Appl. Mech.*, Series E, **30**, 384 (1963).
16. J. P. Lambert and G. H. Jonas, *USA Ballistic Research Laboratories Report No. 1852*, January 1976.
17. D. R. Paul, J. W. Barlow, and H. Keskkula, in *The Encyclopedia of Polymer Science and Technology*, Vol. 12, John Wiley and Sons, Inc., New York, 1988, p. 404.
18. L. E. Nielsen, *Mechanical Properties of Polymers*, Reinhold Publishing Corp., New York, 1962, p. 180.
19. L. H. Van Vlack, *Materials Science for Engineers*, Addison-Wesley Publishing Company, Inc., Reading, MA, 1970, pp. 407-409.
20. D. R. Paul, J. W. Barlow, and H. Keskkula, in *The Encyclopedia of Polymer Science and Technology*, Vol. 12, John Wiley and Sons, Inc., New York, 1988, pp. 417-430.
21. L. H. Sperling, *Introduction to Physical Polymer Science*, John Wiley and Sons, Inc., New York, 1986, pp. 114-116.
22. C. A. Brighton and D. A. Lannon, in *The Encyclopedia of Polymer Science and Technology*, Vol. 8, John Wiley and Sons, Inc., New York, 1987, pp. 417-430.